communications biology

A Nature Portfolio journal

Article

https://doi.org/10.1038/s42003-025-07829-y

Genetically-encoded markers for confocal visualization of single dense core vesicles

Junwei Yu[1,4], Yunpeng Zhang[1,3,4], Kelsey Clements[1], Nannan Chen[2] ✉ & Leslie C. Griffith[1] ✉

Neuronal dense core vesicles (DCVs) store and release a diverse array of neuromodulators, trophic factors, and bioamines. The analysis of single DCVs has largely been possible only using electron microscopy, which makes understanding cargo segregation and DCV heterogeneity difficult. To address these limitations, we develop genetically encoded markers for DCVs that can be used in combination with standard immunohistochemistry and expansion microscopy to enable single-vesicle resolution with confocal microscopy in *Drosophila*.

The release of neuroactive substances in the brain has classically been thought to occur via two distinct pathways. Small-molecule neurotransmitters, packaged into small clear synaptic vesicles (SVs, 30–40 nm diameter), are released at active zones of synapses. In contrast, peptide and neuromodulators are packaged into dense core vesicles (80–200 nm diameter), which fuse extrasynaptically[1]. Neuromodulators play crucial roles in transducing the effects of internal states and external conditions to the brain, making understanding the mechanisms of neuromodulator release essential for understanding how context influences behavior[2].

Co-transmission, the release of multiple neuroactive substances by single cells, introduces another level of complexity. The co-packaging of multiple substances into a single vesicle imposes different constraints on signaling compared to the situation in which a cell can traffic and release each substance independently. Understanding where a neurochemical is released and what other substances are co-released is crucial for comprehending the interactions between synaptic and modulatory pathways. These questions have most often been addressed using techniques with single-vesicle resolution, e.g., single synapse functional data[3] or immuno-electron microscopy[4]. While these techniques can observe specific synapses, they do not allow for a comprehensive examination of the occurrence of co-packaging and co-transmission.

Here, we develop genetic tools for DCV visualization, enabling single DCV resolution with light microscopy when combined with expansion microscopy (ExM)[5] in *Drosophila*. We achieve this by creating a collection of IA2-expressing transgenic lines and lines in which endogenous IA2 is tagged with a fluorescent protein. IA2 family proteins (PTPRN and PTPRN2 in mammals, IDA1 in *C. elegans*, IA2 in *Drosophila*) are trans-membrane proteins that are embedded in DCVs and are expressed in neuroendocrine cells throughout the body, making them excellent markers for DCVs[6].

Results and Discussion

To visualize the extent of endogenous IA2 expression, we used CRISPR/Cas9 to insert monomeric green fluorescent protein (mEGFP) into the *Drosophila IA2* genetic locus to produce a C-terminus fusion (Supplementary Fig. 1a). As would be expected for a DCV marker, we found widespread expression of IA2 in both adult and larval brains (Supplementary Fig. 1b).

To allow cell-specific visualization of DCVs we utilized the GAL4/UAS system[7] (Fig. 1a) and created transgenic lines expressing EGFP-tagged IA2 under control of UAS. *Pigment-Dispersing Factor (PDF)-GAL4*, a driver expressed in peptidergic ventrolateral neurons (LNvs) of the *Drosophila* circadian clock, demonstrated colocalization of EGFP with PDF peptide (Supplementary Fig. 2a). ExM, which increases brain size by about 4.5-fold, and DCVs to about 360-900 nm in diameter, made DCVs visible with light microscopy (Fig. 1f). We found PDF peptide located at the center of IA2-containing circular structures (Supplementary Fig. 2b-c), suggesting that IA2::mEGFP localizes to DCVs which store and release PDF. Notably, in the small LNv projections we did not observe PDF puncta that lacked adjacent IA2 staining. This is the first time that single dense-core vesicles have been visualized by optical microscopy in tissue.

To check whether GAL4-driven expression of IA2::mEGFP affects DCV function, we quantified PDF staining in the projection regions of small LNvs and found there was an increase in PDF signal intensity (Supplementary Fig. 3). This suggests that under normal conditions IA2 levels may be rate-limiting for DCV formation and that IA2::mEGFP is sufficiently functional that its overexpression can increase steady-state DCV levels. Since the protein-tyrosine phosphatase (PTP) region of IA2 is conserved and functionally important, we constructed *UAS-truncated(tr)IA2::mEGFP* lines lacking that domain (Fig. 1a) to block the ability of the transgenic protein to alter DCV levels. Expression of trIA2::mEGFP also labeled single DCVs after expansion (Fig. 1g), but did not change PDF signal intensity (Supplementary Fig. 3), making trIA2::mEGFP a better GAL4-driven DCV marker.

[1]Department of Biology, Volen National Center for Complex Systems, Brandeis University, Waltham, MA, USA. [2]School of Life Science and Technology, Key Laboratory of Developmental Genes and Human Disease, Southeast University, Nanjing, China. [3]Present address: Gempharmatech Co., Ltd, Nanjing, China. [4]These authors contributed equally: Junwei Yu, Yunpeng Zhang. ✉e-mail: nannanchen27@seu.edu.cn; griffith@brandeis.edu

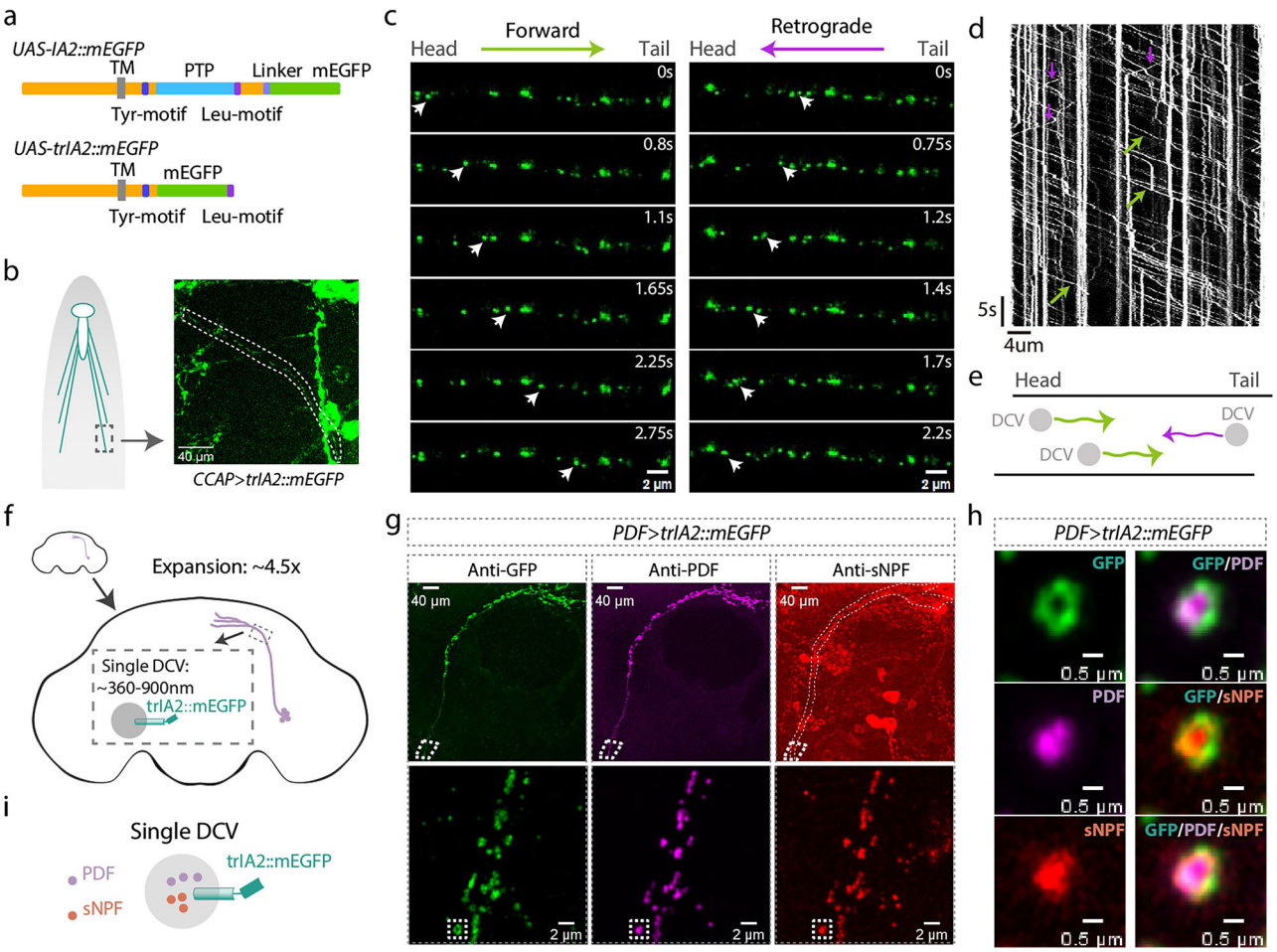

Fig. 1 | Visualizing individual DCVs. a Schematic diagrams of *Drosophila IA2* transgenes: In the *UAS-IA2::mEGFP* fly, mEGFP is fused to the C-terminus of IA2 (upper panel). In the *UAS-trIA2::mEGFP* fly, the C-terminal PTP domain is removed and replaced with mEGFP, followed by IA2's Leu-motif (lower panel). TM: transmembrane domain, PTP: protein-tyrosine phosphatase domain. **b** Cartoon and representative image showing projection (dotted lines) of a trIA2::mEGFP-expressing CCAP neuron. **c** Sequential images showing vesicles (arrowheads) moving from head to tail (left panels) or tail to head (right panels). Scale bar: 2 µm in each panel. **d** Image depicts vesicle movement along the motor neuron projection over time. Right diagonals indicate representative vesicles (green arrows) moving from head to tail, while left diagonals indicate representative vesicles (magenta arrows) moving from tail to head. Vertical lines denote stationary vesicles. **e** Cartoon illustrating relative levels of vesicle movement. **f** Cartoon illustrating the approximately 4.5-fold brain size increase, with 360–900 nm DCVs. PDF and sNPF peptides are co-packaged into the same DCVs. Lower panels of **g** show enlarged images of outlined area in upper panels. **h** shows close-up of the inset in lower panels of **g**. Green: mEGFP, magenta: PDF, red: sNPF in **g**, **h**. Scale bar: 40 µm in upper panels of **g**, 2 µm in lower panels of **g** and 0.5 µm in **h**. **i**, cartoon of co-packaging.

We noticed that nearly all IA2 signals visible in small LNv processes have corresponding PDF staining (Fig. 1g and Supplementary Fig. 2), suggesting that IA2 exclusively labels DCVs and not SVs, much like mammalian PTPRN, which is excluded from SVs[8]. To rule out association between fly IA2 and SVs, we generated an IA2 knock-out strain by deleting the last eight exons of the *IA2* gene. This line was homozygous viable, and adult brains had a dramatic decrease in DCV cargo-positive puncta in small LNv projections, indicating that IA2 enhances but is not required for, DCV function. Importantly, the levels of synaptophysin-labeled SVs in LNvs remained unchanged, confirming that IA2 exclusively affects DCVs (Supplementary Fig. 4a–c). Consistently, immunohistochemical localization of trIA2::mEGFP in motor neuron terminals at the larval neuromuscular junction demonstrates that it does not co-localize with cysteine string protein (CSP), an SV marker (Supplementary Fig. 5). Additionally, cell-specific loss of IA2 indicates that its role in DCV function is cell autonomous (Supplementary Fig. 4d).

In the cytoplasm of neurons, DCVs are dynamic. To determine if IA2 could be used as a marker in live imaging, we examined the projections of larval motor neurons expressing trIA2::mEGFP (Fig. 1b). Use of the transgene provided a bright signal and allowed us to specifically see motor neuron DCVs without background from DCVs in the glia or sensory axons present in body wall nerve. We observed labeled DCVs moving from soma to synaptic regions, as well as a few DCVs moving retrograde (Fig. 1c–e). These results indicate that these genetic reagents can also be used to investigate the mechanisms underlying DCV movement in real-time.

Many neurons, including LNvs[9], express multiple peptides. To determine if our marker could be used to distinguish between co-release from the same DCV and co-transmission via independent DCV populations, we stained adult brains from *PDF>trIA2::mEGFP* animals with antibodies to PDF and sNPF. We found that the peptides located together at the center of single vesicles (Fig. 1g–i). We found a similar situation in the motor neuron of muscle 12 in the third instar larva (Fig. 1b), where CCAP and pBurs co-localize in the same DCVs (Supplementary Fig. 6). These results demonstrate that multiple neuropeptides can be co-packaged into the same DCVs for co-release in both larval and adult *Drosophila* neurons and that IA2 marker transgenes can be used to distinguish between co-release and co-transmission via multiple DCV pools.

Most well-described DCV cargoes are proteinaceous; small molecules involved in fast neuronal communication are primarily released from SVs. Bioamines are an exception to this rule and are known to be packaged in

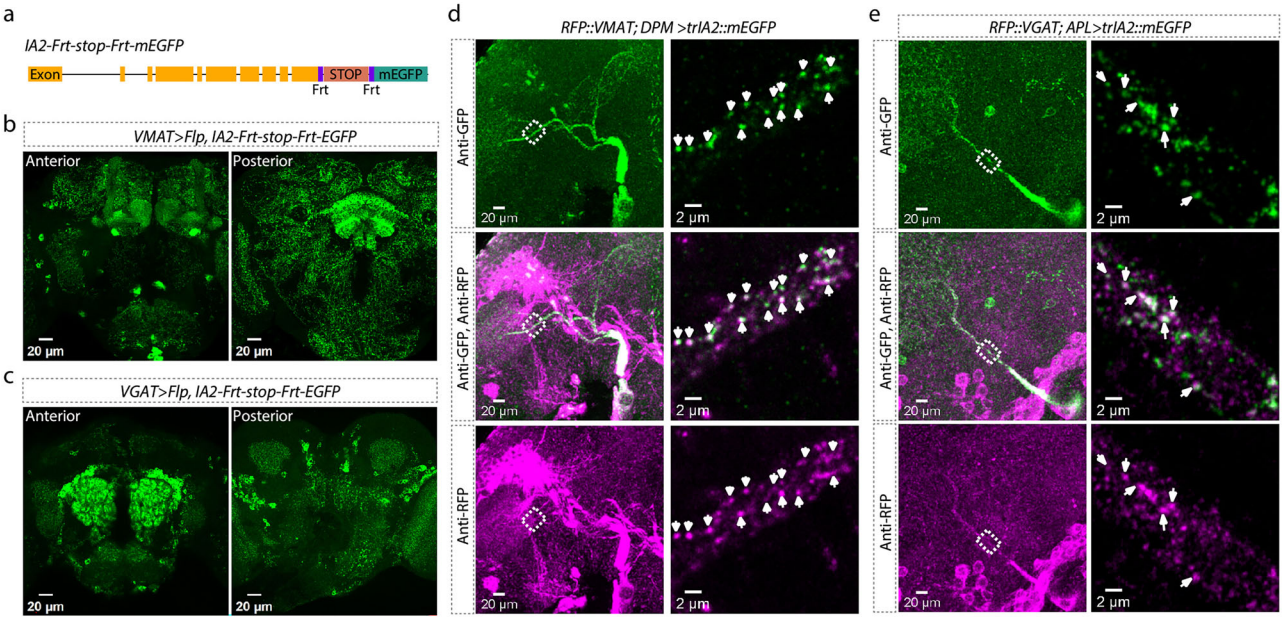

Fig. 2 | Co-localization of DCV IA2 with VMAT and VGAT. a Schematic showing CRISPR insertion of *Frt-stop-Frt-mEGFP* in the 3' end of the *IA2* gene. IA2 expression in VMAT-positive (**b**) and VGAT-positive (**c**) neurons. Left panels show anterior view, right panels show posterior view. Scale bar: 20 µm. **d** Co-localization of RFP::VMAT from endogenous *VMAT* locus with trIA2::EGFP. Left: DPM neuron projections in an expanded fly brain. Right: super-resolution images of the outlined area. Arrowheads indicate DCVs co-labeled by trIA2::mEGFP and RFP::VMAT. Scale bar: 20 µm on left, 2 µm on right. **e** Co-localization of RFP::VGAT[15] with trIA2::EGFP. Left: APL neuron projections in an expanded fly brain. Right: super-resolution images of the outlined area. Arrowheads indicate DCVs co-labeled by trIA2::mEGFP and RFP::VGAT. Scale bar: 20 µm on left, 2 µm on right.

both SVs and DCVs, reflective of their dual roles as synaptic transmitters and extrasynaptic modulators[10,11]. We wondered whether other small-molecule neurotransmitters might also have roles as modulators and be packaged into DCVs. To test this idea, we examined co-localization of IA2::mEGFP with vesicular transporters, proteins that are localized to vesicle membrane and serve to load neurotransmitters into SVs. Each of the main small molecule neurotransmitters requires a different transporter: vesicular monoamine transporter (VMAT) for bioamines, vesicular acetylcholine transporter (VAChT) for acetylcholine, vesicular glutamate transporter (VGluT) for glutamate, and vesicular GABA transporter (VGAT) for γ-aminobutyric acid (GABA). To determine if IA2 was normally present in neurons that release these transmitters, we constructed an *IA2-Frt-stop-Frt-mEGFP* fly strain (Fig. 2a) by inserting an Frt-stop-Frt-mEGFP cassette at the C-terminus of the *IA2* locus. The stop cassette suppresses EGFP tagging unless removed by recombination. Expression of flippase (Flp) cell-specifically fuses the endogenous IA2 protein in *GAL4>Flp* cells with EGFP. We found high levels of endogenous IA2 expression in bioaminergic (*VMAT>Flp*, Fig. 2b), GABAergic (*VGAT>Flp*, Fig. 2c), cholinergic (*VAChT>Flp*, Supplementary Fig. 7a) and glutamatergic (*VGluT>Flp*, Supplementary Fig. 7b) cells.

Since we knew that VMAT was present in some DCVs[11], we examined its co-localization with IA2::mEGFP as a positive control. We first used CRISPR/Cas9 to label endogenous VMAT with RFP (*RFP::VMAT*). We then labeled DCVs with trIA2::mEGFP only in the two bioaminergic dorsal paired medial (DPM) neurons[12]. We found that a substantial number of the trIA2::mEGFP puncta also contained VMAT::RFP, confirming the previous biochemical finding that monoamines can be packaged into DCVs (Fig. 2d and Supplementary Fig. 8a).

GABA is known to be present in DCVs in mammalian adrenal[13]. To determine if GABA can be packaged into DCVs in the *Drosophila* brain, we used trIA2::mEGFP to label the DCVs in the GABAergic anterior paired lateral (APL) neurons[14] on a *VGAT::RFP*[15] background. Though most VGAT::RFP did not colocalize with trIA2::mEGFP, there were clear instances of co-localized signal, indicating that GABA can be packaged into DCVs (Fig. 2e and Supplementary Fig. 8b). The idea that GABA could be neuromodulatory has been around for a while, and it is clear that extrasynaptic signaling by GABA is important for setting circuit tone in both insect and mammalian brains[13,16,17]. These data suggest that DCVs are a potential source of this modulatory GABA.

While synaptic release of small "fast" transmitters like glutamate, acetylcholine and GABA is relatively well characterized, extrasynaptic release of DCVs has been more difficult to study due in part to the greater diversity of vesicle cargos (peptides, bioamines) and the more subtle circuit functions of neuromodulation. Using the genetic tools we developed, researchers can visualize DCVs, track moving DCVs, and observe the co-existence of SVs with DCVs under light microscopy. These tools enable the exploration of a wide variety of questions about the localization and interactions of neurochemical signaling pathways at the whole brain or circuit level.

Methods

Fly strains and husbandry

All flies were raised on a standard cornmeal medium at 25 °C with a 12 h/12 h light cycle. For adult fly experiments, flies were collected at eclosion and aged to 3–5 days before performing experiments. *PDF-GAL4* was kindly provided by Dr. Michael Rosbash, *UAS-ANF::mOrange2* by Dr. Edwin S Levitan, and *UAS-synaptophysin::pHTomato* by Dr. Andre Fiala. *CCAP-GAL4* (#25685), *ChAT-GAL4* (#60317), *VMAT-GAL4* (#66806), *VGluT-GAL4* (#60312), *nos-GAL4* (#64277), and *UAS-Flp* (#4539) were obtained from the Bloomington *Drosophila* Stock Center. *APL-GAL4* (*VT-043924-GAL4*) and *DPM-GAL4* (*VT-064246-GAL4*) were collected from the Vienna Drosophila Resource Center. *VGAT-GAL4* and *RFP::VGAT* were constructed in this lab and described previously[18].

Generation of 10x*UAS-IA2::mEGFP* and 10x*UAS-trIA2::mEGFP* lines

For the *UAS-IA2::mEGFP* fly strain, the IA2 coding region was amplified from a *Canton-S* wildtype fly cDNA library with forward primer TTACTTCAGGCGGCCGCGGCTC GAGATGCCAGCCGTCGGCACT TCTTGC and reverse primer GGATCCACCTCCGCCAG ATCCGCCC

TTCTTCGCCTGCTTCGCCGATTTGGCTG. GFP was amplified from the pJFRC2-10XUAS-IVS-mCD8::GFP plasmids (Addgene Plasmid #26214), and then amino acid A206 was mutated to K to make mEGFP (monomeric enhanced GFP). The primers used are GFP-up forward GGCGGATCTGGCGGAGGTGGATCCATGGTGAGTAAAGGAGAA GAACTTTTCAC, GFP-up reverse GATCTTTCGAAAGCTTAGATTGT GTGGACAG, GFP-down forward CTGTCCACACAATCTAAGCTTTC GAAAGATC and GFP-down reverse AGG TTCCTTCACAAAGATCC TCTAGATTATTTGTATAGTTCATCCATGCCAAGTG. The 10XUAS-IVS-mCD8::GFP plasmid was digested with XhoI (NEB, Cat# R0146S) and XbaI (NEB, Cat# R0145S) restriction enzymes, and the IA2 coding region with the mEGFP fragment were subclone into the plasmid with Gibson assembly method (NEB, Cat# E5510S).

For the *UAS-trIA2::mEGFP* fly strain, the PTP domain and the following fragments of *IA2* were deleted and replaced with mEGFP, followed by the Leu-motif. The primers used are trIA2 forward TTACTTCAGG CGGCCGCGGCTCGAGATGCCAGCCGTCG GCACTTCTTGC, trIA2 reverse ACCATGCCACCGCCGCCCGCTTTG, GFP forward CAAAGC GGGCGGCGGT GGCATGGTGAGTAAAGGAGAAGAACTTTTCAC, GFP reverse1 GCTGCTACCTCCACCC AGGATGGCGTGCACCTCCT CTTTGTATAGTTCATCCATGCCAAG and GFP reverse2 AGTA AGGT TCCTTCACAAAGATCCTCTAGATTAGCTGCTGCTACCTCCACCC AGGATGGC. The fragments were assembled in order and subcloned into the same vector at the same position as that for the UAS-IA2::mEGFP, using the Gibson assembly method (10xUAS-IA2::mEGFP plasmid and 10xUAS-trIA2::mEGFP plasmid in Supplementary Data 1 separately).

These plasmids were verified by sequencing and then injected into *phiC31-attP* flies (Bloomington *Drosophila* stock center, #25710), which have an attP site on the third chromosome to allow targeted integration. The progeny of the injected flies was screened using the w^+ red eye marker and confirmed by GFP staining after being driven by Gal4 strains.

Generation of IA2-Frt-stop-Frt-mEGFP, RFP::VMAT and IA2::mEGFP

To knock in the *Frt-stop-Frt-mEGFP cassette* at the C-terminus of *IA2*, we designed a guide RNA that recognize the endpoint of *IA2* with an online tool (http://targetfinder.flycrispr.neuro.brown.edu/). This guide RNA, which is GCCGAGGACGCCAGCCAAAT, was cloned into a pU6 plasmid (Addgene, #45946) using BbsI restriction enzyme digestion (NEB, Cat# R0539S) and T4 ligase ligation (NEB, Cat #M0202S). Additionally, a donor plasmid (pMC10-IA2-Frt-stop-Frt-mEGFP plasmid in Supplementary Data 1) was created and injected into the Cas9 flies (*y,sc,v; nos-Cas9/CyO;* +/+) along with the gRNA plasmid. Correct integrations were confirmed by PCR and sequencing using primers that bind outside the integrated junction region. The primer pair of left-arm forward CCTTCAGAATCGA CAGTTGGAACGATG and left-arm reverse TCGACTCCGGACTAG CTAGCTTACG was used to determine left arm integration, and the primer pair of right-arm forward ACCATTACCTGTCCACACAATCTAAGC and right-arm reverse GCGATTGACTATAATAC GATACATTTACG TTGC was used to determine right arm integration. We sequenced left arm PCR product with primer of GAGCAAATACTACACATGCAGGGATAC and right arm PCR product with a primer of AAGATCCCAACGAAA AGAGAGACCAC.

Using the same strategy, we knocked in RFP at the N-terminus of VMAT. The guide RNA sequence is GGGCGTCGGCAAGGAGCCAC, and the donor plasmid is shown in Supplementary Data 1. The primers used are left-arm forward ATGCCTGCAGGTCGACTCTA GAGGATCCCA ATTTGTATAGTTCAACCAATTTC, left-arm reverse GGAGGAGGAG GATCA GGAGGAGGAGGATCACAATCATCGACCGATGCGGGC, right-arm forward GACGTCCTC GGAGGAGGCCATTGCGTCGCTAG CCGCTGGTTG, and right-arm reverse CTTAGAAGTC AGAGGCAC GGGCGCGAGATGTGGTATACTGGTACTTCAGCTTTTG. Correct integrations were confirmed by PCR and sequencing using primers that bind outside the integrated junction region.

To get the *IA2::mEGFP* fly strain, we bred *IA2-Frt-stop-Frt-mEGFP* flies with a stable fly line that constantly expresses Flp from the X chromosome. To get the FLP expressing stable line, we crossed *nos-GAL4* (#64277) with *UAS-FLP* (#29731) flies and obtained one recombinant line. We screened progeny of *nos-GAL4, UAS-Flp;; IA2-Frt-stop-Frt-mEGFP* flies and harvested *IA2::mEGFP* fly strains, in which the Frt sequence was used as a soft linker by adding two nucleotides to the beginning of the first Frt site to make it in frame.

Generation of Frt-IA2::mEGFP-Frt and IA2 Null lines

To generate the *Frt-IA2::mEGFP-Frt* fly strain, we used CRISPR/Cas9 to knock in two Frt sites: one in the third intron of the *IA2* gene and another at the end of *IA2*. Two guide RNAs, sgRNA-left GCAAGGAGTTAGTG-CAACTG and sgRNA-right GCCGAGGACGCCAGCCAAAT, were designed accordingly and cloned into pU6 plasmids (Addgene, #45946) respectively. In the donor plasmid (Frt-IA2::mEGFP-Frt plasmid in Supplementary Data 1), mEGFP is inserted at the C terminus of IA2, and followed by the second Frt site. The donor plasmid was co-injected into Cas9 flies (*y,sc,v; nos-Cas9/CyO;* +/+) along with the gRNA plasmids. We used GFP fluorescence to screen larval progenies, and then confirmed by PCR and sequencing. Correct integrations were confirmed by PCR and sequencing using primers that bind outside the integrated junction region. The primer pair of left-arm forward GCATTCAGGTCAC GTCTC TGTTGG and left-arm reverse CCAATCTTCACCAGCTTCCACACAC was used to determine left arm integration. The primer pair of right-arm forward ACCATTACCTGTCCAC ACAATCTAAGC and right-arm reverse GCGATTGACTATAATACGATACATTTACGTTGC was used to determine right arm integration.

After obtaining the *Frt-IA2::mEGFP-Frt* fly, we crossed it with *nos-GAL4, UAS-FLP* flies, screened the progeny with GFP loss first, and confirmed by PCR and sequencing. The primer pair of forward TCGACTC ATGATATCCTTCCTAATGG and reverse TCCTCCTACTGACAA TCTCGTGAAG was used to amplify the deletion area. The PCR product was sequenced using the primer AGTCTCAAAGAGATTAAGCCAG AGCC, and the IA2 sequence is provided in Supplementary Data 1. We successfully harvested the *IA2 Null* mutant fly strain. This line is homozygous viable.

Immunohistochemistry and image processing

To dissect and stain the brains of adult and larval flies, we followed the protocols from Janelia (www.janelia.org/project-team/flylight/protocols). Briefly, the brains were dissected in S2 solution and then fixed in 2% paraformaldehyde solution for 55 minutes at room temperature (RT). The brains were then washed four times, 10 minutes each time, with 0.5% phosphate-buffered saline containing Triton X-100 (PBST). Following the washes, the brains were blocked with 5% goat serum in PBST solution for 1.5 hours at RT. The samples were then incubated in primary antibody solution for 4 hours at RT with continued incubation at 4 °C over 2-3 nights. Subsequently, samples were washed three times for 30 mins each with 0.5% PBST and incubated in secondary antibody over two nights. The same washing process was performed afterward. Some samples then underwent the expansion protocol as described below, while others are fixed in 4% PFA for an additional 4 hours at RT and mounted in Vectashield mounting medium (Vector Laboratories).

To visualize NMJs on larval body walls, wandering third instar larvae were dissected in cold HL3.1 solution (NaCl 70 mM, KCl 5 mM, $CaCl_2$ 0.1 mM, $MgCl_2$ 20 mM, $NaHCO_3$ 10 mM, Trehalose 5 mM, Sucrose 115 mM, HEPES 5Mm; osmolarity: 395.4 mOsm, pH7.1–7.2) and then fixed in 4% PFA for 10 mins at RT. The samples were then washed in PBST for 3×10 minutes and incubated in primary antibody solution overnight. Following this, the samples were washed again and incubated in secondary antibody solution for another night. After a final wash for 3 × 30 mins, the mounting process was performed.

The primary antibodies used were rabbit anti-GFP (1:1000; Thermo Fisher Scientific, A-11122), rabbit anti-RFP (1:200; Takara, 632496), mouse

anti-GFP (1:200; Sigma-Aldrich, 11814460001), chicken anti-GFP (1:500; Invitrogen, A10262), mouse anti-PDF (1:200; Developmental Studies Hybridoma Bank; PDF C7-c), mouse anti-Csp antibody (1:100; Developmental Studies Hybridoma Bank, DCSP-1 (ab49)), rabbit anti-CCAP (1:500; Jena Bioscience; ABD-033), rabbit anti-sNPF (1: 500; a gift from Dr. Jan Veenstra, Universite de Bordeaux, France), and mouse anti-pBurs (1:500; a gift from Benjamin White, National institute of Health; originally from Dr. Aaron Hsueh, Stanford University). The secondary antibodies used were Alexa Fluor 488 anti-chicken antibody (Invitrogen, A-11039), Alexa Fluor 488 anti-mouse antibody (Invitrogen, A-10680), Alexa Fluor 488 anti-rabbit antibody (Invitrogen, A-11008), and Alexa Fluor 568 anti-rabbit (Invitrogen, A-11011). Alexa Fluor 635 anti-mouse antibody (Invitrogen, A-31574) and Alexa Fluor 635 anti-rabbit antibody (Invitrogen, A-31576), all at 1:200 dilutions. For NMJs staining, Alexa Fluor 488-conjugated anti-GFP antibody (1:250; Invitrogen, A-21311) was used.

Images were captured using a Leica SP5 confocal microscope with either a 20x or 60x objective lens, except for the NMJs images, which were acquired on a Zeiss LSM880 Airy Scan Fast Confocal System using a 63x objective lens. The images from Leica SP5 were then processed and analyzed using ImageJ Fiji software[19], while the Airy Scan images underwent deconvolution using Huygens software.

ExM sample preparation

The brain samples for expansion microscopy were prepared as previously described[20]. After dissecting and staining the brains, they were incubated in AcX solution (0.1 mg/ml) for more than 24 hours at RT in the dark. Brains were then washed three times with PBS solution and incubated in a gelling solution for 45 minutes on ice in the dark. Gel chambers were constructed by placing two strips of tape approximately 3–4 cm apart on a glass slide. Brains were placed into the gel chambers and incubated in a gelling solution at 37 °C for 2 hours. After incubation, the brains were trimmed away from the gelling solution and submerged in a digestion buffer for 24 hours at room temperature in the dark. Finally, brains were washed with an excess volume of ddH_2O at room temperature more than three times, 20 mins each time. The samples were then prepared for imaging with a ZEISS LSM 880 Airyscan microscope with a 63x objective.

Live imaging of DCVs and data analysis

Third instar larval brains were dissected in ice-cold HL3 medium. The brains were then transferred to an imaging chamber containing fresh HL3 saline, which was continuously supplied to the chamber during the recording process. Images of motor neuron projections were captured at 12 Hz with a 63X Multi-Immersion lens under a ZEISS LSM 880 Airyscan microscope with the AiryScan FAST model. For the analysis of dense core vesicle trafficking, we used the Kymograph plugin in the imageJ[19] (Fiji) as described previously[21].

Statistical analysis and Reproducibility

Prism 9 software was used for statistical analysis. Data were tested for normality and then analyzed with either a parametric or non-parametric test as appropriate. Biological replicates are indicated by a N.

Reporting summary

Further information on research design is available in the Nature Portfolio Reporting Summary linked to this article.

Data availability

Source data for the graphs in Supplementary Figs. 3 and 4 can be found in Supplementary Data 2. All other data supporting the findings of this study are available from the corresponding author upon reasonable request.

Received: 26 September 2024; Accepted: 26 February 2025;
Published online: 07 March 2025

References

1. Edwards, R. H. Neurotransmitter release: variations on a theme. *Curr. Biol.* **8**, R883–885 (1998).
2. Flavell, S. W., Gogolla, N., Lovett-Barron, M. & Zelikowsky, M. The emergence and influence of internal states. *Neuron* **110**, 2545–2570 (2022).
3. Kim, S., Wallace, M. L., El-Rifai, M., Knudsen, A. R. & Sabatini, B. L. Co-packaging of opposing neurotransmitters in individual synaptic vesicles in the central nervous system. *Neuron* **110**, 1371–1384.e1377 (2022).
4. Woodruff, E. A. 3rd, Broadie, K. & Honegger, H. W. Two peptide transmitters co-packaged in a single neurosecretory vesicle. *Peptides* **29**, 2276–2280 (2008).
5. Karagiannis, E. D. & Boyden, E. S. Expansion microscopy: development and neuroscience applications. *Curr. Opin. Neurobiol.* **50**, 56–63 (2018).
6. Torii, S. Expression and function of IA-2 family proteins, unique neuroendocrine-specific protein-tyrosine phosphatases. *Endocr. J.* **56**, 639–648 (2009).
7. Brand, A. H. & Dormand, E. L. The GAL4 system as a tool for unraveling the mysteries of the *Drosophila* nervous system. *Curr. Opin. Neurobiol.* **5**, 572–578 (1995).
8. Nishimura, T., Kubosaki, A., Ito, Y. & Notkins, A. L. Disturbances in the secretion of neurotransmitters in IA-2/IA-2beta null mice: changes in behavior, learning and lifespan. *Neuroscience* **159**, 427–437 (2009).
9. Johard, H. A. et al. Peptidergic clock neurons in Drosophila: ion transport peptide and short neuropeptide F in subsets of dorsal and ventral lateral neurons. *J. Comp. Neurol.* **516**, 59–73 (2009).
10. McDonald, A. J. Functional neuroanatomy of monoaminergic systems in the basolateral nuclear complex of the amygdala: Neuronal targets, receptors, and circuits. *J. Neurosci. Res.* **101**, 1409–1432 (2023).
11. Grygoruk, A. et al. The redistribution of Drosophila vesicular monoamine transporter mutants from synaptic vesicles to large dense-core vesicles impairs amine-dependent behaviors. *J. Neurosci.* **34**, 6924–6937 (2014).
12. Lee, P. T. et al. Serotonin-mushroom body circuit modulating the formation of anesthesia-resistant memory in Drosophila. *Proc. Natl. Acad. Sci. USA* **108**, 13794–13799 (2011).
13. Harada, K. et al. GABA Signaling and Neuroactive Steroids in Adrenal Medullary Chromaffin Cells. *Front Cell Neurosci.* **10**, 100 (2016).
14. Liu, X. & Davis, R. L. The GABAergic anterior paired lateral neuron suppresses and is suppressed by olfactory learning. *Nat. Neurosci.* **12**, 53–59 (2009).
15. Chen, N. et al. Widespread posttranscriptional regulation of cotransmission. *Sci. Adv.* **9**, eadg9836 (2023).
16. Keles, M. F., Hardcastle, B. J., Stadele, C., Xiao, Q. & Frye, M. A. Inhibitory Interactions and Columnar Inputs to an Object Motion Detector in Drosophila. *Cell Rep.* **30**, 2115–2124.e2115 (2020).
17. Arslan, A. Extrasynaptic delta-subunit containing GABA(A) receptors. *J. Integr. Neurosci.* **20**, 173–184 (2021).
18. Chen, N. Z., et al. Widespread posttranscriptional regulation of cotransmission. *Sci. Adv.* eadg9836 (2023).
19. Schindelin, J. et al. Fiji: an open-source platform for biological-image analysis. *Nat. Methods* **9**, 676–682 (2012).
20. Chen, F., Tillberg, P. W. & Boyden, E. S. Expansion microscopy. *Science* **347**, 7 (2015).
21. Inoshita, T., Hattori, N. & Imai, Y. Live Imaging of Axonal Transport in the Motor Neurons of Drosophila Larvae. *Bio Protoc.* **7**, e2631 (2017).

Acknowledgements

This work was supported by R21NS096414 and R01NS122970 to LCG. Stocks obtained from the Bloomington Drosophila Stock Center (NIH P40OD018537) were used in this study.

Author contributions

J.Y., Y.Z. and L.C.G. designed the experiments. J.Y., Y.Z., N.C. and K.C. generated reagents and carried out experiments. J.Y., Y.Z. and N.C. analyzed the data. LCG and NC wrote and edited the manuscript.

Competing interests

The authors declare no competing interests.

Additional information

Supplementary information The online version contains supplementary material available at https://doi.org/10.1038/s42003-025-07829-y.

Correspondence and requests for materials should be addressed to Nannan Chen or Leslie C. Griffith.

Peer review information *Communications Biology* thanks Martin Pauli and the other anonymous, reviewer(s) for their contribution to the peer review of this work. Primary Handling Editors: Periklis Pantazis and Dario Ummarino. A peer review file is available.